Ferroelastic order parameter and W' domain walls in $A_4LiH_3(SO_4)_4$ ($A=NH_4$, Rb, K)

B. Mróz
Institute of Physics, A. Mickiewicz University, Umultowska 85, 61-614, Poznań, Poland

S. M. Kim and B. M. Powell
AECL, Chalk River Laboratories, Chalk River, Ontario, Canada KOJ 1JO

H. Kiefte
Department of Physics, Memorial University, St. John's, Newfoundland, Canada A1B 3X7

R. L. Donaberger
Department of Physics, McMaster University, Hamilton, Ontario, Canada L8S 4MI

(Received 20 May 1996; revised manuscript received 27 January 1997)

High-resolution neutron powder diffraction was used to study the lattice parameters of three crystals: $Rb_4LiH_3(SO_4)_4$ (RLHS), deuterated ammonium $(NH_4)_4LiH_3(SO_4)_4$ (ALHS), and $K_4LiH_3(SO_4)_4$ (KLHS) in a temperature range from 5 to 250 K. For RLHS and ALHS a continuous ferroelastic phase transition $4F2$ was detected at 134 and 234 K, respectively. KLHS was found to show monoclinic symmetry in the whole temperature region studied. Using the structural data obtained, it was possible to calculate the temperature behavior of spontaneous strain e_S and its components $(e_{11}-e_{22})$ and e_{12}. This allowed the calculation of the possible temperature changes in the orientation of W' domain walls. The ''pinning energy'' modification of the free energy expansion was introduced to explain the discrepancy between the measured temperature dependence of the order parameter and that expected in the Landau approximation. [S0163-1829(97)14417-4]

I. INTRODUCTION

Almost all crystals of the general formula $A_4LiH_3(BO_4)_4$, where $A=$Rb, NH_4, K and $BO_4=SO_4$ or SeO_4, undergo structural phase transitions[1–11] from the prototype tetragonal point group 4 to the low-temperature ferroelastic point group 2. The $4F2$ transition is accompanied by the appearance of W'-type domain walls in the ferroelastic phase, softening of the elastic constant c_{2S} on both sides of the transition, and the onset of an elastic order parameter, namely, spontaneous strain e_S of the form $e_S=(e_{11}-e_{22})+e_{12}$.[12,13]

Recently, a number of papers have described investigations of crystals of this family: for example, the results of Brillouin scattering studies of $Rb_4LiH_3(SO_4)_4$ (RLHS) and $K_4LiH_3(SO_4)_4$ (KLHS) have been reported.[3,6] A characteristic feature of RLHS revealed by these studies was the incomplete softening of the elastic constant c_{2S}. Both the incomplete softening of c_{2S} and the crossover behavior of the $P_S(T)$ function have been successfully explained in terms of a theoretical model based on the mean-field approximation.

The ferroelasticity in ammonium $(NH_4)_4LiH_3(SO_4)_4$ (ALHS) has been reported by Polomska *et al.*[14] who observed ferroelastic domain walls below 230 K. The ferroelastic character of the phase transition in ALHS was later confirmed by studies of their thermal and elastic properties, carried out using the torsion vibration technique[15] and in Brillouin experiments.[11] With the latter technique it was possible to measure the temperature dependence of the elastic constant coupled to the order parameter and then calculate the temperature behavior of the soft elastic constant c_{2S}. Unlike in RLHS, the constant c_{2S} of ALHS vanishes at T_c on cooling, consistent with a Curie-Weiss law.

Data on the ferroelastic domain structure of ALHS and RLHS were provided by studies performed with a polarizing microscope.[16] The observed domain pattern consisted of two types of mutually perpendicular walls rotated about the Z axis by about 33° (ALHS) and 35° (RLHS) (see Fig. 1). From our observations it appeared that these walls did not rotate on cooling the sample down to 100 K below T_c. On the other hand, Knite *et al.*[17] found a slight reorientation of the ALHS walls (by about 0.02°/K). The possible orientation of W' walls was also calculated for ALHS using the results of Brillouin scattering studies.[16] From the known components of the elastic moduli coupled to the spontaneous strain, it was found that T_c domains were inclined at 33° to the X axis. In the case of KLHS, the ferroelasticity was not confirmed and the only indication of a low-temperature phase transition was a slight change in slope of the velocity of L phonons versus temperature at about 115 K.[16]

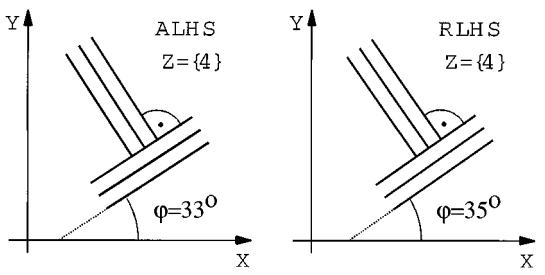

FIG. 1. Schematic drawing of W' domain wall orientation for ALHS and RLHS just below T_c.

Raman scattering was used to study the lattice vibrations in single crystals of KLHS and RLHS.[10] For RLHS, it was found that two modes of B symmetry in the paraelastic phase showed some critical behavior. The most interesting was the band at 31 cm^{-1}, which showed slight softening while approaching T_c from above. In addition, the polar modes of A and E symmetries were found to be better separated for KLHS than those for RLHS, which may be due to a higher dispersion of TO and LO mode frequencies. This occurs when long-range forces are favored over short-range ones. Such dominance of the long-range forces may be the lattice-stabilizing factor that makes the formation of the ferroelastic phase in KLHS difficult or perhaps impossible.

The structural data of $A_4LiH_3(SO_4)_4$ crystals indicate that their common high-temperature prototype symmetry is the $P4_1$ tetragonal space group, whereas the low-temperature ferroelastic phase is characterized by a monoclinic distortion in the XY plane (space group $P2_1$). The results of an x-ray investigation of the crystals have been restricted to a few temperatures of the prototype and low-temperature phases (see Zuniga *et al.*[9]) or the temperature ranges of the phase investigated were too narrow to obtain credible fits of critical exponents.[18]

There are a few methods for the determination of the absolute value of spontaneous strain appearing in the ferroelastic phase:[19] (i) direct measurements of elastic hysteresis loop, (ii) thermal expansion studies, and (iii) structural investigation. The sensitivity of the first method depends strongly on the form of spontaneous strain, and in the case when e_s is a two-component quantity, the reliability of such measurements becomes questionable. The same reservation applies to the second method. The powder diffraction method is most suitable for the determination of the multicomponent order parameter provided that the sample is powdered finely enough to exclude the effect of its domain structure on the quality of the recorded spectra.

In this paper we report results of high-resolution neutron powder diffraction studies of $A_4LiH_3(SO_4)_4$ crystals (where A=Rb, NH_4, and K). The technique used in our experiment allowed the lattice parameter studies in a very wide temperature range (5–250 K). With the results obtained we determined the temperature behavior of the spontaneous strain e_s and its components ($e_{11}-e_{22}$ and e_{12}). The correlation between the domain wall orientation and the temperature changes of spontaneous deformation is discussed. We suggest that KLHS has monoclinic symmetry at room temperature; however, the temperature range of the prototype phase is still an open question.

II. EXPERIMENTAL PROCEDURE

Crystals of ALHS, RLHS, and KLHS were grown isothermally at 310 K by the dynamic method from the acid aqueous solution (pH$\leqslant 1$) of the appropriate initial salts in stoichiometric proportion.[20] Since $(NH_4)_4LiH_3(SO_4)_4$ contains 19 hydrogen atoms per molecule, it is impossible to obtain good quality coherent scattering data. To be able to make the analysis reliable, it was necessary to grow fully deuterated samples. Full replacement of H by D atoms was achieved by the use of D_2SO_4, $(ND_4)_2SO_4$, D_2O, and Li_2CO_3. No significant isotopic effect was detected in the phase transition temperature, lattice parameters, differential thermal-analysis (DTA) signals, and elastic properties of the deuterated samples.

High-resolution neutron powder diffraction data have been collected for ALHS, RLHS, and KLHS in wide temperature ranges. The main point of interest was the temperature behavior of the lattice parameters in the ferroelastic phase. The DUALSPEC C2 Powder Diffractometer, located at the NRU Reactor at Chalk River Laboratories, was used in the studies presented. The 800-wire detector subtended a scattering angle of 80° with 0.1° wire spacing. The wavelength of the neutrons selected by a Si(531) monochromator was 1.505 Å. Neutron diffraction profiles were measured for scattering angles from 5° to 121° in 0.05° steps. The data were analyzed with the Rietvald analysis program GSAS.[21]

III. EXPERIMENTAL RESULTS AND DISCUSSION

The discussion of our results of neutron scattering studies in ALHS and RLHS crystals will be based on the RLHS crystal as the example, since for this material there is also extensive x-ray data. The approach proposed for this material has been successfully applied, with a slight modification, to ALHS. Finally, we shall present the results of structural investigations of KLHS for which a ferroelastic phase transition has not been observed in the studied temperature range.

The room-temperature structure of the RLHS compound has been determined by Zuniga *et al.*[9] and Pietraszko and Lukaszewicz[8] from single-crystal x-ray diffraction as well as optical activity measurements. The authors found that at room temperature its structure is tetragonal with space group $P4_1$. In analyzing the present neutron diffraction data, the atomic positions determined by Zuniga *et al.* were used as the initial values. Since the positions of the three H atoms could not be determined by the x-ray diffraction measurements,[9] we have determined these positions from the Rietveld analysis on the present neutron diffraction data on the tetragonal phase RLHS. In the Rietveld fit, it was not possible to vary the temperature factors for the different atoms, and thus we assumed that the low-temperature temperature factors for the constituent atoms in RLHS are proportional to those determined by x-ray diffraction at room temperature averaged over the same type of atoms, and only the temperature factor for the H atoms was varied. In this fit, the lattice parameters, background function, scattering angle zero position, profile parameters, and the scale factor were varied. Attempts to further refine the positions of Li or O atoms, previously determined by the x-ray diffraction measurements by Zuniga *et al.*,[9] were not successful. For temperatures between 140 and 167 K, good fits to the data (R_w=2.90–3.19 %) were obtained for the tetragonal space group $P4_1$. Since the single-crystal x-ray data on RLHS by Zuniga *et al.*[9] indicated the presence of a small fraction of a phase with space group $P4_3$, the data were also analyzed including a component with $P4_3$ space group. However, inclusion of this component worsened the fit, indicating that the structure is a single phase with space group $P4_1$. The fractional atomic coordinates and isotropic mean-square displacements in the tetragonal phase RLHS at 170 K are given in Table I.

We have also attempted to determine the low-temperature

TABLE I. Fractional atomic coordinates and isotropic mean-square displacements (Å^2), $U_{iso}=\frac{1}{3}\langle u^2\rangle$, in tetragonal phase RLHS at 170 K.

	x	y	z	U_{iso}
Rb(1)	0.0645(2)	0.8853(2)	0.71800(5)	0.0163(5)
Rb(2)	0.3652(2)	0.3840(2)	0.70491(5)	0.0163(5)
Rb(3)	0.5291(2)	0.9751(2)	0.08343(5)	0.0163(5)
Rb(4)	0.2271(2)	0.4808(2)	0.07356(4)	0.0163(5)
S(5)	0.4620(4)	0.1245(4)	0.20459(9)	0.0123(5)
O(6)	0.575(1)	0.255(1)	0.2250(3)	0.0213(5)
O(7)	0.377(1)	0.209(1)	0.1618(3)	0.0213(5)
O(8)	0.319(1)	0.077(1)	0.2332(3)	0.0213(5)
O(9)	0.561(1)	−0.022(1)	0.1862(3)	0.0213(5)
S(10)	0.4107(3)	0.1222(4)	0.45631(9)	0.0123(5)
O(11)	0.341(1)	0.253(1)	0.4867(3)	0.0213(5)
O(12)	0.256(1)	0.028(1)	0.4343(3)	0.0213(5)
O(13)	0.510(1)	−0.006(1)	0.4793(3)	0.0213(5)
O(14)	0.506(1)	0.206(1)	0.4197(3)	0.0213(5)
S(15)	0.0361(4)	−0.0053(4)	0.08669(8)	0.0123(5)
O(16)	0.170(1)	0.108(1)	0.0664(3)	0.0213(5)
O(17)	0.130(1)	−0.154(1)	0.1088(3)	0.0213(5)
O(18)	−0.059(1)	0.087(1)	0.1221(3)	0.0213(5)
O(19)	−0.087(1)	−0.068(1)	0.0522(3)	0.0213(5)
S(20)	0.5380(4)	0.6973(4)	0.33303(9)	0.0123(5)
O(21)	0.393(1)	0.599(1)	0.3503(3)	0.0213(5)
O(22)	0.489(1)	0.845(1)	0.3064(3)	0.0213(5)
O(23)	0.627(1)	0.774(1)	0.3766(3)	0.0213(5)
O(24)	0.668(1)	0.588(1)	0.3102(3)	0.0213(5)
Li(25)	0.279(2)	0.869(2)	0.2704(7)	0.0143(5)
H(26)	0.293(4)	0.311(4)	0.1686(9)	0.014(8)
H(27)	0.831(4)	0.277(4)	0.1216(9)	0.014(8)
H(28)	0.075(4)	0.802(4)	0.1511(9)	0.014(8)

monoclinic structure of RLHS from the observed neutron powder diffraction intensities. The atomic positions in the tetragonal unit cell were used as the initial data. As the tetragonal space group $P4_1$ contains a fourfold screw axis along the z axis, the unit cell contains four layers of RLHS molecules. The monoclinic space group $P2_1$, on the other hand, allows only a twofold screw axis along this z axis. Since the monoclinic unit cell also contains four RLHS molecules, as shown by the present neutron diffraction measurements, the lowering of the screw axis symmetry from 4 to 2 leads to the second- and fourth-layer atoms being slightly displaced from their tetragonal positions.

We assumed that in the monoclinic structure the positions of the second and fourth-layer atoms constituting the RLHS molecule transform as a rigid body. Various possible displacements of the rigid body origin as well as various possible rotations of these rigid molecules were then tried. A significant improvement in the fit ($R_w=4.42$ versus $R_w=4.58$) was obtained when the origin of the tetragonal coordinate system is moved by $-0.045(10)$ Å along the x axis, $-0.020(9)$ Å along the y axis and $-0.137(16)$ Å along the z axis. The fractional atomic coordinates and isotropic mean-square displacements in the monoclinic phase RLHS at 5 K are given in Table II.

In Figs. 2 and 3 we present the lattice parameters and

TABLE II. Fractional atomic coordinates and isotropic mean-square displacements (Å^2), $U_{iso}=\frac{1}{3}\langle u^2\rangle$, in monoclinic phase RLHS at 5 K.

	x	y	z	U_{iso}
Rb(1)	0.6160(2)	0.3652(2)	−0.0451(5)	0.010(2)
Rb(2)	1.1147(2)	1.0645(2)	−0.0320(5)	0.010(2)
Rb(3)	1.2271(2)	0.4808(2)	0.0736(4)	0.010(2)
Rb(4)	0.5291(2)	0.9751(2)	0.0834(5)	0.010(2)
S(5)	1.1245(4)	0.5380(4)	−0.0454(9)	0.008(2)
O(6)	1.255(1)	0.425(1)	−0.0250(3)	0.013(2)
O(7)	1.209(1)	0.623(1)	−0.0882(3)	0.013(2)
O(8)	1.077(1)	0.681(1)	−0.0168(3)	0.013(2)
O(9)	0.978(1)	0.439(1)	−0.0638(3)	0.013(2)
S(10)	0.5893(3)	0.8778(4)	−0.0437(9)	0.008(2)
O(11)	0.659(1)	0.747(1)	−0.0133(3)	0.013(2)
O(12)	0.744(1)	0.972(1)	−0.0657(3)	0.013(2)
O(13)	0.490(1)	1.006(1)	−0.0207(3)	0.013(2)
O(14)	0.494(1)	0.794(1)	−0.0803(3)	0.013(2)
S(15)	0.6973(4)	0.4620(4)	0.0830(9)	0.008(2)
O(16)	0.599(1)	0.607(1)	0.1003(3)	0.013(2)
O(17)	0.845(1)	0.511(1)	0.0564(3)	0.013(2)
O(18)	0.774(1)	0.373(1)	0.1266(3)	0.013(2)
O(19)	0.588(1)	0.332(1)	0.0602(3)	0.013(2)
S(20)	1.0361(4)	0.9947(4)	0.0867(8)	0.008(2)
O(21)	1.170(1)	1.108(1)	0.0664(3)	0.013(2)
O(22)	1.130(1)	0.846(1)	0.1088(3)	0.013(2)
O(23)	0.941(1)	1.087(1)	0.1221(3)	0.013(2)
O(24)	0.913(1)	0.932(1)	0.0522(3)	0.013(2)
Li(25)	0.8480(2)	0.7052(2)	0.0246(7)	0.009(2)
H(26)	0.293(4)	0.311(4)	−0.081(1)	0.009(2)
H(27)	0.831(4)	0.277(4)	0.122(1)	0.009(2)
H(28)	0.075(4)	0.802(4)	0.151(1)	0.009(2)
Rb(29)	0.629(1)	0.618(1)	0.200(1)	0.010(2)
Rb(30)	−0.070(1)	1.112(1)	0.213(1)	0.010(2)
Rb(31)	0.513(1)	1.228(1)	0.319(1)	0.010(2)
Rb(32)	0.019(1)	0.527(1)	0.329(1)	0.010(2)
S(33)	0.456(1)	1.125(1)	0.200(1)	0.008(2)
O(34)	0.569(2)	1.257(2)	0.220(1)	0.013(2)
O(35)	0.371(2)	1.209(2)	0.157(1)	0.013(2)
O(36)	0.313(2)	1.077(2)	0.229(1)	0.013(2)
O(37)	0.555(2)	0.980(2)	0.182(1)	0.013(2)
S(38)	0.116(1)	0.588(1)	0.202(1)	0.008(2)
O(39)	0.247(2)	0.658(2)	0.232(1)	0.013(2)
O(40)	0.022(2)	0.742(2)	0.180(1)	0.013(2)
O(41)	−0.012(2)	0.487(2)	0.225(1)	0.013(2)
O(42)	0.200(2)	0.493(2)	0.165(1)	0.013(2)
S(43)	−0.001(1)	1.034(1)	0.332(1)	0.008(2)
O(44)	−0.114(2)	1.167(2)	0.312(1)	0.013(2)
O(45)	0.148(2)	1.129(2)	0.354(1)	0.013(2)
O(46)	−0.093(2)	0.938(2)	0.367(1)	0.013(2)
O(47)	0.062(2)	0.911(2)	0.298(1)	0.013(2)
S(48)	0.532(1)	0.699(1)	0.328(1)	0.008(2)
O(49)	0.387(2)	0.599(2)	0.346(1)	0.013(2)
O(50)	0.483(2)	0.846(2)	0.302(1)	0.013(2)
O(51)	0.621(2)	0.776(2)	0.372(1)	0.013(2)
O(52)	0.662(2)	0.590(2)	0.306(1)	0.013(2)
Li(53)	0.289(1)	0.848(1)	0.270(1)	0.009(2)
H(54)	0.684(4)	0.293(4)	0.164(2)	0.009(2)
H(55)	0.717(4)	0.834(4)	0.367(2)	0.009(2)
H(56)	0.192(4)	1.074(4)	0.396(2)	0.009(2)

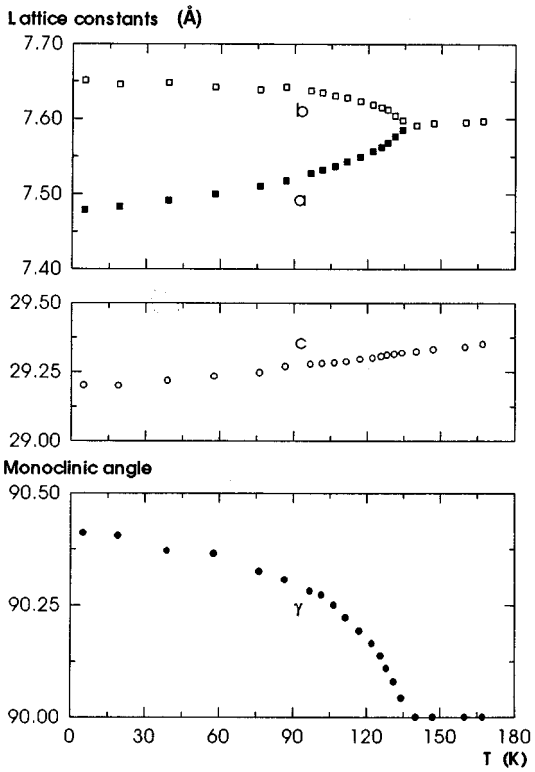

FIG. 2. Lattice parameters of RLHS vs temperature.

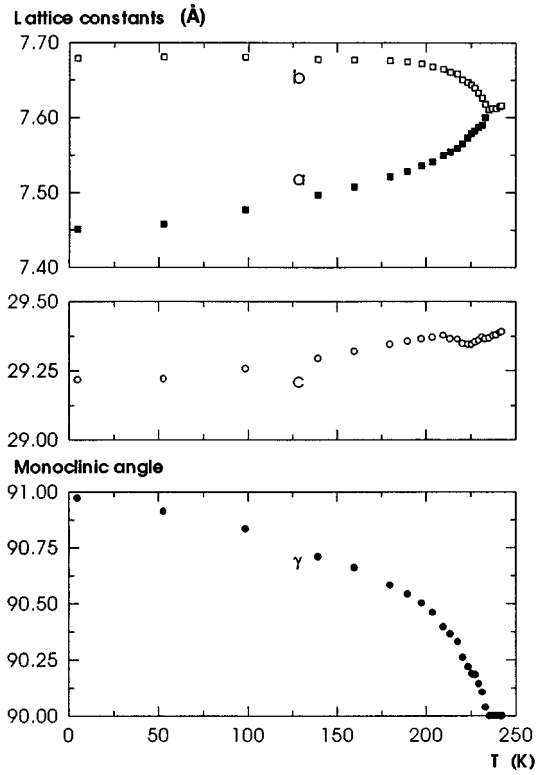

FIG. 3. Lattice parameters of deuterated ALHS vs temperature.

monoclinic angles of RLHS and ALHS calculated from our neutron spectra. The standard deviations are less than the diameter of the circles representing the data. For the ALHS crystal, the ND_4 molecule was approximated as an atom located at the Rb site with the scattering length corresponding to the ND_4 molecule. This approximation is adequate for our purposes since the size of the ND_4 molecule (2.06 Å) is comparable with that (1.47 Å) of the Rb atom. It is evident that both materials undergo a continuous phase transition with a typical splitting of the a and b lattice constants below T_c. The monoclinic angle γ of RLHS and ALHS shows a critical behavior reaching the values of 0.40° and 0.70°, respectively, at 60 K below T_c. In the case of ALHS, a slight anomaly of the c-lattice constant at T_c was observed.

For KLHS both tetragonal (space group $P4_1$) and monoclinic (space group $P2_1$) fits were tried for all temperatures between 4.2 and 250 K. In the tetragonal fit, atomic positions were assumed to be the same as those for RLHS. In the monoclinic fit, the second- and fourth-layer atoms, i.e., the second- and fourth-layer KLHS molecules, as shown in Fig. 1 of Zuniga *et al.*,[9] were assumed to be displaced slightly from their tetragonal positions as a rigid body as was done for the Rb compound.

Significant improvement in the fit was obtained for the monoclinic symmetry when the second- and fourth-layer molecules, shown in Fig. 1 of Zuniga *et al.*, were rotated counterclockwise as a rigid body about the tetragonal x axis by 1.7°. The reliability factors for this monoclinic structure ($R_W = 5.25-6.64$ %) are significantly better than those for the tetragonal structure ($R_W = 5.90-7.29$ %) for all temperatures between 4.2 and 250 K. The degree of this counterclockwise rotation about the tetragonal x axis appeared to be rather insensitive to temperature: We obtained $1.68° \pm 0.08°$ for 105 K and $1.65° \pm 0.08°$ for 125 K in the Rietvald analysis. The observed temperature dependences of the lattice parameters a, b, and c and the monoclinic angle γ are shown in Fig. 4.

From a comparison of these results with the results of Brillouin scattering studies of KLHS,[6] it may be concluded that this crystal in low temperatures undergoes an isostructural phase transition inside the monoclinic phase. However, the existence of the paraelastic tetragonal prototype is questionable since our thermal expansion studies performed at higher temperatures did not reveal any critical behavior.[22]

IV. SPONTANEOUS STRAIN CALCULATION

Let us calculate the spontaneous strain resulting from the group-subgroup relation for the case of a $4 \rightarrow 2$ ferroelastic transition. The symmetry elements of point groups 4 and 2 are

$$4 \quad \{4, 4^2=2, 4^3, 4^4=1\} \quad \text{paraelastic},$$

$$2 \quad \{2, 2^2=1\} \quad \text{ferroelastic}. \tag{1}$$

The number of elements of paraelastic (n_p) and ferroelastic (n_f) groups gives the expected number of the orientation states of the low-temperature phase. In our case $n_p/n_f = 2$. The strain tensor of the monoclinic group 2 has the form

$$e(s_1) = \begin{pmatrix} e_{11} & e_{12} & 0 \\ & e_{22} & 0 \\ & & e_{33} \end{pmatrix}. \tag{2}$$

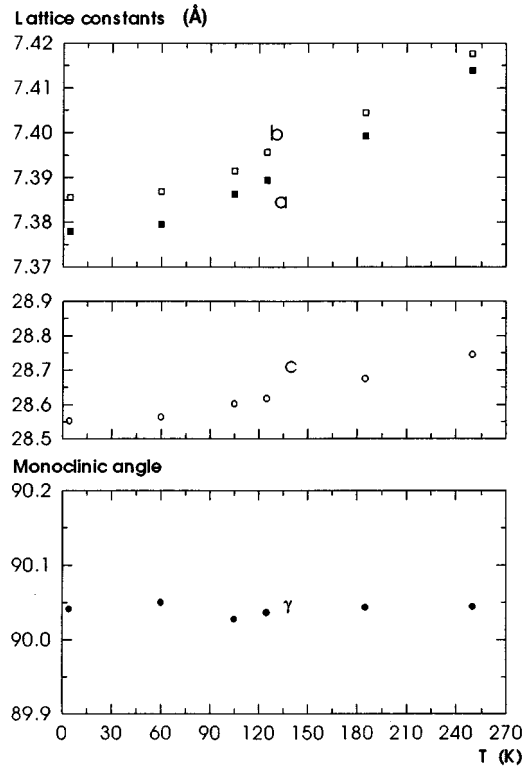

FIG. 4. Lattice parameters of KLHS vs temperature.

To find the possible form of the spontaneous strain tensor, we have to calculate the mean value of the strain tensor by acting on the tensor $e(s_1)$ which is lost at T_c. Acting on $e(s_1)$ with the four-fold axis matrix, we get the second possible tensor of deformation:

$$e(s_2)=\begin{pmatrix} e_{22} & -e_{12} & 0 \\ & e_{11} & 0 \\ & & e_{33} \end{pmatrix}. \tag{3}$$

The spontaneous strain tensor $e_s(s_k)$ of the k-orientation state is calculated as,

$$e_s(s_k)=e(s_k)-\tfrac{1}{2}[e(s_1)+e(s_2)], \tag{4}$$

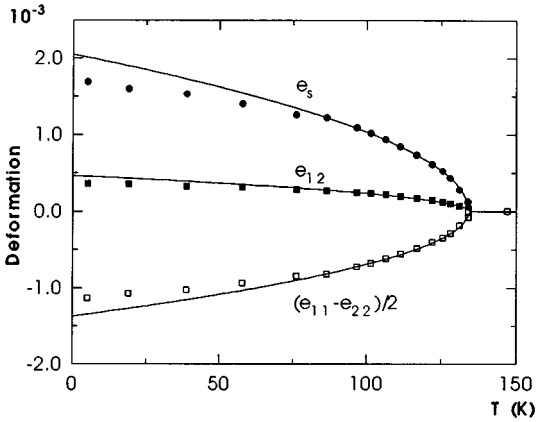

FIG. 5. Temperature dependence of the spontaneous strain e_S and its components, RLHS.

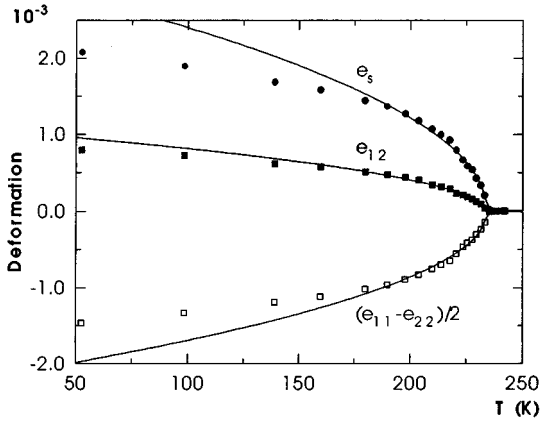

FIG. 6. Temperature dependence of the spontaneous strain e_S and its components, deuterated ALHS.

where the last term in Eq. (4) is the mean value of the strain. Using this expression, we get the forms of spontaneous strain e_s for the orientation states s_1 and s_2:

$$e_s(s_1)=\begin{pmatrix} \dfrac{e_{11}-e_{22}}{2} & e_{12} & 0 \\ & -\dfrac{e_{11}-e_{22}}{2} & 0 \\ & & 0 \end{pmatrix}, \tag{5}$$

$$e_s(s_2)=\begin{pmatrix} -\dfrac{e_{11}-e_{22}}{2} & -e_{12} & 0 \\ & \dfrac{e_{11}-e_{22}}{2} & 0 \\ & & 0 \end{pmatrix}. \tag{6}$$

The value of spontaneous strain is given by $e_s=\Sigma_{i,j}\sqrt{e_{ij}^2}$. Taking into account that $e_{12}^s=\tan[(\gamma-90)/2]$, we have e_s for the $4F2$ ferroelastic phase transition:

$$e_s=\sqrt{\tfrac{1}{2}(e_{11}-e_{22})^2+2e_{12}^2}. \tag{7}$$

With the results given in Figs. 1 and 2, we calculated the temperature dependences of e_s and its components ($e_{11}-e_{22}$) and e_{12}. The plots [see Fig. 5 (RLHS) and Fig. 6 (ALHS)] were fitted (solid line) with the critical exponent $\frac{1}{2}$. The fitting parameters of the function $e=A(T-T_c)^{1/2}$ are given in Table III. As is evident from Figs. 5 and 6, the mean-field approximation holds very well in a wide temperature range for both crystals.

In the last column of Table III, we give the approximate temperature range ΔT_L of the ferroelastic phase where the Landau fit diverges from experimental data. This will be

TABLE III. Fitting parameters of the function $e_i=A(T-T_c)^{1/2}$ for RLHS and ALHS.

	T_c (K)		A (10^{-4})	ΔT_L (K)
		e_{12}	4.02±0.01	60
RLHS	134.3±0.2	$\frac{1}{2}(e_{11}-e_{22})$	−11.9±0.2	45
		e_s	17.7±0.3	45
		e_{12}	7.1±0.1	110
ALHS	233.8±0.3	$\frac{1}{2}(e_{11}-e_{22})$	−14.6±0.3	60
		e_s	20.6±0.3	60

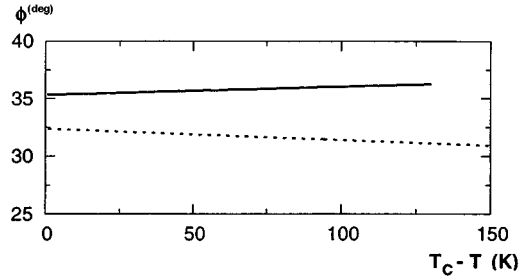

FIG. 7. Temperature changes in W' domain wall orientation: solid line, RLHS; dashed line, deuterated ALHS.

used in the next section where we discuss the correlation between the domain wall orientations and temperature changes of spontaneous deformation.

V. W' DOMAIN WALLS IN ALHS AND RLHS

According to the classification given by Sapriel,[12] one may distinguish two types of ferroelastic domain walls: W-type walls, which appear when the crystal loses the minor crystallographical plane at T_c and which are crystallographically prominent planes of fixed indices, and W'-type walls, whose orientation depends on the actual values of the different components of spontaneous strain.

In general, the orientation of any type of ferroelastic domain walls between two orientation states s_1 and s_2 is given by[12]

$$[e_s(s_1)_{ij}-e_s(s_2)_{ij}]x_i x_j=0, \tag{8}$$

where $e_s\ (s_k)_{ij}$ are the components of the spontaneous tensor of the k-orientation state. From Eqs. (5), (6), and (8), we have

$$\cdot\left(\frac{e_{11}-e_{22}}{2}\right)x^2+2e_{12}xy-\left(\frac{e_{12}-e_{22}}{2}\right)y^2=0. \tag{9}$$

Combining Eq. (9) with $y=Ax$, we finally have the form of the domain wall equation for the $4F2$ phase transition:

$$y=\left(\frac{b}{e}\pm\sqrt{\left(\frac{b}{e}\right)^2+1}\right)x, \tag{10}$$

where $b=e_{12}$ and $e=\frac{1}{2}(e_{11}-e_{22})$.

According to Eq. (10), the orientation of W' domain walls may be temperature dependent. The necessary condition for such a dependence is, of course, the difference between the critical exponents of b and e components. In the case when both b and e show the same critical behavior, their temperature dependences cancel each other and Eq. (10) becomes temperature independent.

As follows from Table III and Figs. 5 and 6, the Landau fits of $(e_{11}-e_{22})$ and e_{12} hold very well for temperatures down to 45 K below T_c for both ALHS and RLHS.

In Fig. 7 we have plotted the expected temperature dependence [calculated from Eq. (10)] of the angle between the tetragonal x axis and the actual direction of W' walls for ALHS and RLHS crystals. For the temperatures close to T_c, the results obtained are in good agreement with direct observations of domain structure in those crystals.[16] From Fig. 7 it appears that the expected rotation is about 1°. The only difference is that for ALHS one expects the slight lowering of the angle, whereas RHLS shows the opposite behavior.

The results obtained for ALHS are also in good agreement with the results of calculations of the pure-mode direction. As reported in Ref. 16, the pure-mode direction is at 33° with respect to the x axis and decreases by a few degrees when the crystal is cooled far from the transition. The question can be asked whether W' walls can undergo reorientation and what factors can inhibit this process.

VI. PINNING OF THE DOMAIN WALLS TO THE IMPURITIES

We shall now discuss the influence of the crystal defects on the temperature dependence of the ferroelastic order parameter. In this discussion we shall resort to the procedure used in interpreting the shape of the double-hysteresis loop in ferroelastic $LiCsSO_4$,[23] involving the introduction of a pinning energy to the energy balance:

$$E_{\rm pin}(e_s)=k\int_0^{e_s}de_s, \tag{11}$$

where k is proportional to the average density of pinning sites and the characteristic pinning energy of the site for a domain wall. Here e_s denotes the actual strain energy exhibited by the sample, in contrast to e_s^0, which is the so-called antihysteretic strain responsible for lossless reorientation processes. In such a case the elastic deformation energy equals the lossless contribution minus the loss due to hysteresis:

$$\int e_S d\sigma_{\rm eff}=\int e_S^0(\sigma_{\rm eff})d\sigma_{\rm eff}-k\int\left(\frac{de_S}{d\sigma_{\rm eff}}\right)d\sigma_{\rm eff}, \tag{12}$$

where $\sigma_{\rm eff}$, the effective stress, includes both externally applied stress σ and the mean-field contribution, so that

$$\sigma_{\rm eff}\approx\sigma+\alpha e_S, \tag{13}$$

with α being the mean-field constant.

Differentiating Eq. (12) with respect to $\sigma_{\rm eff}$ yields

$$e_S=e_S^0+\delta k\left(\frac{de_S}{d\sigma_{\rm eff}}\right), \tag{14}$$

where $\delta=1$ if $\sigma_{\rm eff}$ increases in the positive direction and $\delta=-1$ if $\sigma_{\rm eff}$ increases in the negative direction. This ensures that the pinning opposes changes in reorientation. By applying the approach of Ref. 23 we finally get the approximate expression for spontaneous strain:

$$e_S\cong e_S^0+\frac{\delta k}{2A_2}, \tag{15}$$

where A_2 is the soft elastic constant c_{2S}. It is obvious that the pinning modification of e_S given by Eq. (15) changes the temperature behavior of e_S.

Since e_S is a two-component quantity, it can be concluded that if the orientation of W' walls changes with temperature, the crystal defects must affect the temperature dependence of the components of e_S to a different degree. This is particu-

larly well illustrated in Fig. 6 where e_{12} (proportional to the monoclinic angle) shows the temperature dependence with the exponent $\frac{1}{2}$ over almost the whole temperature range studied, whereas the temperature change of $\frac{1}{2}(e_{11}-e_{12})$ reveals less critical behavior. This may indicate that the linear spontaneous deformation is more sensitive to the presence of defects in the material than the shear component.

The latter problems will be discussed in more detail in the work under preparation.

VII. SUMMARY

We have reported neutron scattering studies of three crystals from the family of materials with composition $A_4LiH_3(SO_4)_4$ where $A=NH_4$, Rb, and K. Our experiments measured the lattice parameters of these crystals over a very wide temperature range from 5 K. From the results it was possible to calculate the spontaneous strain e_S and its components for ALHS and RLHS. The temperature changes of the orientation of W' walls were calculated to be about 1° (deg) at $T_C-T=100$ K. It was shown that W' walls may rotate, remaining perpendicular to each other only when the components of e_S appearing in the wall equation have different critical behavior. The analysis of the equations for W' walls given by Sapriel[12] at different ferroelastic phase transitions indicates that the above conclusion must be generally valid for all transitions characterized by a multicomponent order parameter. The effect of crystal defects on the temperature behavior of spontaneous deformation is also discussed. It has been shown that the introduction of the pinning energy to the free energy causes a decrease in the critical exponent of e_S. The experimentally observed differences in the temperature dependence of the spontaneous deformation components e_{12} and $e_{11}-e_{22}$ suggest that the normal deformation can be more sensitive to the presence of defects than the shear deformation.

ACKNOWLEDGMENTS

This work has been partially supported by State Committee for Scientific Research (KBN) Grant No. 2 P302 036 06. We also wish to acknowledge the Natural Science and Engineering Research Council grant for this work.

[1] T. Krajewski, T. Brêczewski, P. Piskunowicz, and B. Mróz (unpublished).
[2] M. Polomska and F. Smutny, Phys. Status Solidi B **154**, K103 (1988).
[3] J. Minge and T. Krajewski, Phys. Status Solidi A **109**, 193 (1988).
[4] T. Wolejko, G. Pakulski, and Z. Tylczyñski, Ferroelectrics **81**, 1979 (1988).
[5] P. Piskunowicz, T. Brêczewski, and T. Wolejko, Phys. Status Solidi A **114**, 505 (1989).
[6] B. Mróz and R. Laiho, Phys. Status Solidi A **115**, 575 (1989).
[7] B. Mróz, H. Kiefte, M. J. Clouter, and J. A. Tuszyñski, J. Phys. Condens. Matter **3**, 5673 (1991).
[8] A. Pietraszko and K. Lukaszewicz, Z. Krystallogr. **185**, 564 (1988).
[9] F. J. Zuniga, G. Extebarria, G. Madariaga, and T. Brêczewski, Acta Crystallogr. C **46**, 1199 (1990).
[10] B. Mróz, M. Kaczmarski, H. Kiefte, and M. J. Clouter, J. Phys. Condens. Matter **4**, 7515 (1992).
[11] B. Mróz, H. Kiefte, M. J. Clouter, and J. A. Tuszyñski, Ferroelectrics **152**, 337 (1994); J. Phys. Condens. Matter **5**, 6377 (1993).
[12] J. Sapriel, Phys. Rev. B **12**, 5128 (1975).
[13] N. Boccara, Ann. Phys. (N.Y.) **47**, 40 (1964).
[14] M. Polomska, A. Pawlowski, A. Smutny, and J. Wolak (unpublished).
[15] B. Mróz, P. Piskunowicz, A. Pawlowski, and T. Krajewski, Ferroelectrics **159**, 155 (1994).
[16] S. Mielcarek, Z. Tylczyñski, P. Piskunowicz, and B. Mróz, Ferroelectrics **172**, 287 (1995).
[17] M. Knite, W. Schranz, A. Fuith, and H. Warhanek, J. Phys. Condens. Matter **5**, 9099 (1993).
[18] A. Pietraszko, M. Polomska, and A. Pawlowski, Izv. Akad. Nauk SSSR, Ser. Fiz. **55**, 529 (1991).
[19] E. K. M. Salje, *Phase Transitions in Ferroelastic and Co-Elastic Crystals* (Cambridge University Press, Cambridge, England, 1990).
[20] Crystals have been grown at Crystal Physics Division, Institute of Physics, A. Mickiewicz University, Poznañ, Poland.
[21] A. C. Larson and R. B. von Dreele (unpublished).
[22] P. Piskunowicz and B. Mróz (unpublished).
[23] J. A. Tuszyñski, B. Mróz, M. Kiefte, and M. J. Clouter, Ferroelectrics **77**, 111 (1988).